Eur Biophys J (1992) 21, 357–362

European Biophysics Journal

Application of dynamic light scattering to studies of protein folding kinetics

Klaus Gast*, Gregor Damaschun, Rolf Misselwitz, and Dietrich Zirwer

Max-Delbrück-Centrum für Molekulare Medizin, Robert-Rössle-Strasse 10, O-1115 Berlin, Germany

Received May 26, 1992/Accepted in revised form September 16, 1992

Abstract. The applicability of dynamic light scattering to studies of the kinetics of unfolding and refolding reactions of proteins is discussed and demonstrated experimentally. The experimental set-up and the data acquisition and data evaluation schemes that have been optimized for kinetic experiments are described. The relationship of the signal-to-noise ratio to the minimum data acquisition time that is needed to obtain results of sufficiently high precision is discussed. It turns out that the attainable time resolution is of the order of a few seconds for proteins with molar masses of about 50,000 $g \cdot mol^{-1}$ and concentrations of 1 $g \cdot l^{-1}$. Thus, DLS is too slow to follow conformational changes in the subsecond region, but it is useful for studies of unfolding-refolding reactions of proteins that proceed with time constants in the range of seconds or minutes. This is demonstrated by investigations of the kinetics of the cold denaturation of 3-phosphoglycerate kinase from yeast.

Key words: Dynamic light scattering – Stokes' radius – Protein-folding kinetics – Cold denaturation – Yeast 3-phosphoglycerate kinase

Introduction

Dynamic light scattering (DLS) has become a standard technique for measurements of the translational diffusion coefficient D_T of macromolecules and other submicron particles in solution. This allows a rapid and non-invasive estimation of the molecular size by means of the Stokes' radius R_S that can be calculated from D_T via the Stokes-Einstein equation $R_S = kT/6\pi\eta D_T$ (k Boltzmann's constant, T absolute temperature, η solvent viscosity). The physical basis of the method and its application to biomacromolecular systems are well documented (Cummins and Pike 1974; Chu 1974; Pecora 1985; Schmitz 1990; Harding et al. 1992).

In particular, DLS has been successfully applied to monitor changes in the molecular size of proteins upon denaturation and renaturation (Nicoli and Benedek 1976; Gast et al. 1986; Damaschun et al. 1991). The understanding of the pathway of protein folding has received much attention during the past decade. Today, the mechanisms of in-vivo folding are only partly elucidated. To understand at least some particular steps of the folding path, in-vitro unfolding/refolding experiments are of considerable importance (Jaenicke 1987, 1991). Kinetic experiments play an essential role in these investigations, especially in the detection of intermediate states. Until now, kinetic data are mostly obtained by spectroscopic methods. Therefore, one is very interested in a direct access to geometrical data by measuring the radius of gyration by X-ray scattering or the Stokes' radius by DLS. However, the geometrical radius of gyration can only be derived from the hydrodynamic Stokes' radius if the ratio $\varrho = R_g/R_S$ is known (Damaschun et al. 1991). The value of ϱ depends on the molecular conformation and varies between $(3/5)^{1/2}$ for spheres and 1.55 for Gaussian coils (Tanford 1961; Damaschun et al. 1991).

DLS measurements of time-dependent processes have been reported for various biomacromolecular systems. Typical examples are the aggregation of insulin molecules (Dathe et al. 1990; Sluzky et al. 1991), experiments monitoring the crystallization of lysozyme (Mikol et al. 1989; Georgalis et al. 1992), antigen-antibody reactions (Deverill and Lock 1983) and changes of the size distribution of lipid vesicles (Gast et al. 1982). The time constants of these processes were of the order of minutes, hours or days. To the best of our knowledge, direct measurements of time-dependent changes in the molecular size of poteins via R_S during unfolding and refolding reactions have not been reported up to now. According to spectroscopic investigations (Kuwajima et al. 1988), the time constants of these reactions are in the range of subsecond regions up to minutes or hours. Thus, the feasibility of

* *Correspondence to:* K. Gast

Abbreviations: DLS: dynamic light scattering; PGK: 3-phosphoglycerate kinase; EDTA: ethylenediamine tetraacetic acid; GuHCl: guanidine hydrochloride; DTT: dithiothreitol

time-resolved measurements of R_S by DLS and particularly the limit of time resolution that can be reached have to be considered. In general, for most physical methods, such as spectroscopic methods (CD, fluorescence, EPR, NMR), X-ray scattering and total intensity light scattering, the measurement time can be minimized by improving the experimental conditions. For example, the use of synchrotron radiation in X-ray scattering has drastically reduced the data acquisition time, thus allowing one to follow structural changes in the millisecond time range (Laggner et al. 1991). The situation is quite different in the case of DLS. The statistical error in the measured time-autocorrelation function is of the order of $(\tau_c/T_A)^{1/2}$ under optimum experimental conditions. This means that the data acquisition time T_A needed to obtain adequate data for precise estimations of D_T depends on the correlation time $\tau_c = 1/(q^2 D_T)$ itself, where q is the scattering vector. In spite of this general limitation, the experimental procedure has to be optimized with respect to efficient data acquisition, transient storage and data evaluation to perform kinetic experiments with sufficient time resolution and precision. We describe herein a DLS apparatus that was designed mainly for this purpose. As an example of application, we report on changes of the molecular size of 3-phosphoglycerate kinase (PGK) from yeast upon cold denaturation. Cold denaturation of PGK has been demonstrated by Privalov and co-workers using microcalorimetric and spectroscopic techniques (Griko et al. 1989; Privalov 1990). In addition to steady state measurements of the Stokes' radius in the temperature region of cold denaturation, we have performed experiments on the unfolding and refolding kinetics, following the time course of the Stokes' radius after a temperature jump. On the basis of these investigations, we want to demonstrate the usefulness of kinetic DLS measurements on the one hand and the theoretical and practical limitations on the other.

Experimental

Essential components of the DLS spectrometer

The optical part of the spectrometer consists of an argon-laser ILA-120 (Carl-Zeiss Jena, FRG) operating at the wavelength $\lambda = 514.5$ nm, the thermostated cell holder and the detection system. The latter two components are mounted on a modified X-ray goniometer HZG 4 (Praezisionsmechanik Freiberg GmbH, FRG). The homodyne time-autocorrelation functions $G^{(2)}(\tau_l)$ are calculated for L delay times τ_l by a laboratory built multibit multiple-τ correlator (see below). The correlator is on-line coupled with a PC/AT. The PC is equipped with a transputer-board ALV-800 (ALV Laser Vertriebsgesellschaft mbH, Langen, FRG) for fast data evaluation using the program CONTIN (Provencher 1982 a, b). During a kinetic experiment, N_E correlation functions are calculated and stored on the hard disk or a floppy disk. T_A is the data acquisition time for each correlation function, and hence $T_E = N_E \cdot T_A$ is the total experiment time. To render possible short times T_A, an efficient real-time correlation system is required. Furthermore, to avoid large redundant data sets and long data evaluation times, especially in performing the inverse Laplace transformation by CONTIN, the number of data points L should be kept small. This means that the L lag times τ_l must be distributed on an appropriate time grid to ensure an optimum information content. Some details of a correlation system that meets these requirements are described below.

Correlation technique

The photon correlator calculates the unnormalized correlation function

$$G^{(2)}(\tau_l) = \sum_{i=1}^{N} n(t_i)\, n(t_i + \tau_l)/N \qquad (1)$$

at L discrete lag times τ_l. $n(t_i)$ is the number of photon pulses counted within the sample time T at time t_i. In general, the lag time increment and the sample time are identical. Normalization, leading to

$$g^{(2)}(\tau_l) = G^{(2)}(\tau_l)/\bar{n}^2, \qquad (2)$$

is performed by an on-line coupled computer. $\bar{n} = \sum_{i=1}^{N} n(t_i)/N$ is the average count rate and N the total number of samples. Correlation techniques used in dynamic light scattering are described by Schätzel (1987, 1992).

Using modern electronic circuits, nearly ideal multibit, real-time correlators of moderate expense can be built up. Such correlators are able to sample photon pulses in a 4 bit or 8 bit data format and to perform the multiplications and additions according to (1) in parallel for all l. To cover a large range of delay times, it is convenient to use a multiple-τ spacing for τ_l by doubling the lag time increment after 8 or 16 subsequent channels. Working with a fixed grid of delay times allows the construction of a very compact correlator (Schätzel 1992; ALV-5000 manual, ALV Laser Vertriebsgesellschaft mbH, Langen, FRG).

For our purpose, we have developed a multibit correlator with a flexible lag time spacing. A schematic diagram is shown in Fig. 1. It is built up of a data sampling and control unit and a number of correlation units, each consisting of 15 correlation channels with a constant lag time increment T_j and one monitor channel. The T_j are

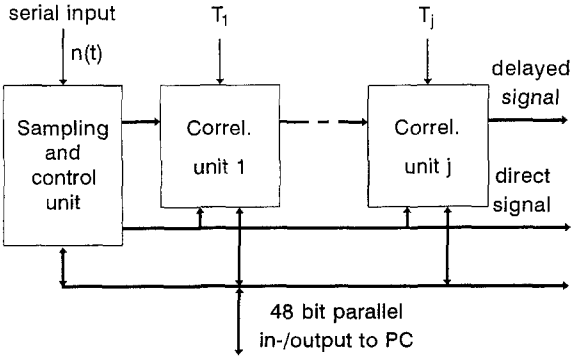

Fig. 1. Schematic representation of the photon correlation system

multiples of 2 of the pre-selectable basic sample time T (T: 10^{-7} s ... 10^{-3} s) and can be programmed to form a correlator with either a linear or a flexible multiple-τ grid ($T_j = T \cdot 2^{r_j}$, $r_j = 0, 1, 2, \ldots$). In this way, the delay times τ_l can be positioned at time regions where most information can be obtained.

The essential electronic component of each correlation channel is a multiplier/accumulator circuit (MAC) ADSP 1010-B (Analog Devices, USA) that is able to form the product of two 16 bit integer numbers and to add the result to the content of an internal 35 bit register within 60 ns. Accordingly, the minimum sample time is 100 ns. The direct and the delayed signal have a data format of 8 bit (255 levels), which provides sufficient resolution and dynamic range. To link two correlation units, an accumulator at the end of the internal delay register adds r_{j+1}/r_j samples with T_j to get a sample for times T_{j+1}. The content of each monitor channel $\bar{n}_j = \sum_{i=1}^{N} n_j(t_i)/N$ is used for adequate normalization

$$g^{(2)}(\tau_l) = G^{(2)}(\tau_l)/(\bar{n} \cdot \bar{n}_j) \tag{3}$$

of the individual parts of the correlation function. This scheme is called symmetric normalization (Schätzel et al. 1988). The physical layout of the correlator allows one to calculate two correlation functions at 135 delay times simultaneously. However, single autocorrelation functions with 75 delay times are used for the present purpose.

Signal-to-noise considerations

The problem of noise in photon correlation has been treated by several authors (Jakeman et al. 1971; Schätzel 1983, 1990; Kojro 1990). To follow relative changes of R_S between 10% and 50%, mostly observed upon unfolding or refolding of proteins, the error in the estimated Stokes' radius should not exceed 1%. Therefore, we seek the data acquisition time T_A, which is necessary to obtain such a precision for a given photon count rate and a correlation time τ_c. The photon count rate can be expressed either by counts per sample time, $\bar{n}$, or by counts per correlation time, r, where $r = \bar{n}/\gamma$ and $\gamma = T/\tau_c$. Following Jakeman et al. (1971) the variance of the estimator of $g^{(2)}(\tau)$ can be expressed for Gaussian-Lorentzian light and $\gamma \ll 1$ as

$$\begin{aligned} \mathrm{Var}\,[g^{(2)}(\tau)] = (N\gamma)^{-1}\,[&(1/2)(1 + 8\exp(-x) \\ &- \exp(-2x)(5 + 2x)) \\ &+ (2/r)(1 + \exp(-x))^2 \\ &+ (1 + \exp(-x))/(r^2\gamma)] \end{aligned} \tag{4}$$

Our experimental situation is consistent with the particular model used by Jakeman et al. (1971), where $g^{(2)}(\tau)$ adopts the from $g^{(2)}(\tau) = 1 + \exp(-x)$, with $x = 2\tau/\tau_c$. This means that the correlation function decays exponentially with a dominant correlation time τ_c, which is determined by the translational diffusion of the protein molecules in the present case. Frequently, the linewidth parameter $\Gamma = 1/\tau_c = q^2 D_T$ is used (Jakeman et al. 1971). The scattering vector q is given by $q = (4\pi n/\lambda)\sin(\theta/2)$, where n is the index of refraction of the solution, λ the wavelength of laser light and θ the scattering angle. $N \cdot T$ is equal to the data acquisition time T_A. According to (4), the variance is proportional to the ratio $\tau_c/T_A = (N\gamma)^{-1}$ in any case. Two limiting situations should be considered. In the ideal case of a high photon flux ($r \gg 1$), the variance is independent of r because the first term in (4) dominates. In the "shot noise limit" ($r \ll 1$), the last term in (4) is dominant. The variance is then proportional to r^{-2}. This means that the acquisition time to obtain a certain statistical error is prolonged approximately by a factor $1/r$. In addition to analytic expressions for the normalized standard deviation of the linewidth parameter $(\mathrm{Var}\,\Gamma/\Gamma^2)^{1/2}$ for special cases, Jakeman et al. (1971) have given results of numerical computations in a graphical form. These results can be used for estimations of the acquisition time T_A, which is necessary to obtain a certain standard deviation in Γ (or $D_T = \Gamma/q^2$), e.g. 1% in our case. For a protein with a molar mass of 50000 g · mol^{-1}, a protein concentration of 1 g · l^{-1} and a laser power of 0.4 W one can expect $\tau_c = 4 \cdot 10^{-5}$ s and a photon count rate of 10^5 s^{-1}. With these data and a sample time $T = 2 \cdot 10^{-6}$ s we get $\gamma = 0.05$, $\bar{n} = 0.2$, $r = 4$. Using the results of the computations of Jakeman et al. (1971), we find $N = 8 \cdot 10^5$ or $T_A = 1.6$ s. This tells us that the time resolution of DLS experiments of this kind is of the order of a few seconds. $(\mathrm{Var}\,\Gamma/\Gamma^2)^{1/2}$ becomes independent of r for $r > 10$. With our experimental value $r = 4$ we cannot expect a remarkable increase in the signal-to-noise ratio or shorter measurement times by increasing the laser power or the protein concentration. The shortest experimental data acquisition time used by us was $T_A = 4.2$ s.

Sample preparation

Yeast 3-phosphoglycerate kinase (EC 2.7.2.3) was purchased from Sigma Chemical Co., USA. The ammonium sulphate precipitated protein was dissolved in 20 mM sodium phosphate, pH 6.5, 10 mM ethylenediamine tetraacetic acid (EDTA), 0.7 M guanidine hydrochloride (GuHCl), 1 mM dithiothreitol (DTT) and then dialyzed exhaustively against the same buffer at room temperature. The sample was then applied to a FPLC-Superose 12 column (Pharmacia, Sweden). Only peak fractions were taken for the DLS measurements. PGK concentrations were determined photometrically using $A^{1\%}_{1\,\mathrm{cm}} = 4.95$ at 280 nm (Adams et al. 1985). The molecular homogeneity of the protein was tested before and after the DLS measurements in 15% sodium dodecyl sulphate polyacrylamid gels according to (Laemmli 1970). Lysozyme (Sigma Chemical Co., USA) was prepared in the same manner in 0.3 M glycine-HCl buffer, pH 2.2 containing 0.15 M NaCl.

All DLS measurements were made at a scattering angle of 90 deg. using fluorescence micro flow-through cells with a sample volume of 100 µl (Hellma, FRG). The solvent and the protein solutions were filtered either through 20 nm pore-size filters (Biotage Europe, U.K.) or 100 nm pore-size filters (Sartorius GmbH, FRG) directly into the scattering cells.

Table 1. Stokes' radii of yeast PGK under different conditions. Native conditions refer to 20 mM sodium phosphate, pH 6.5, 10 mM EDTA, 1 mM DTT. The buffer under conditions b) and c) differs only by the addition of GuHCl

Condition	R_S [nm]
a) native, 20 °C	2.97 ± 0.04
b) 0.7 M GuHCl, 30 °C	3.01 ± 0.04
c) 0.7 M GuHCl, 5 °C	5.03 ± 0.07

Results and discussion

Steady state unfolding-refolding experiments

Yeast PGK consists of 415 amino acids. The molar mass calculated from the amino acid composition is $M = 44\,574\ \mathrm{g \cdot mol^{-1}}$. According to X-ray crystallographic studies (Watson et al. 1982), the protein consists of two domains of similar size. In order to detect any changes in the molecular dimensions connected with destabilizing or denaturing conditions, we have first measured D_T and R_S in the absence of GuHCl at 20 °C. We obtained the translational diffusion coefficient extrapolated to zero concentration and corrected to standard conditions $D^0_{20,w} = (7.21 \pm 0.1) \cdot 10^{-7}\ \mathrm{cm^2 \cdot s^{-1}}$. The corresponding Stokes' radius is $R_S = (2.97 \pm 0.04)$ nm. The concentration dependence of D_T in 20 mM sodium phosphate, pH 6.5, 10 mM EDTA was found to be very weak ($k_D \approx 0.8\ \mathrm{cm^3 \cdot g^{-1}}$).

PGK is somewhat destabilized in the presence of 0.7 M GuHCl, thus shifting the low temperature unfolding transition to easily attainable temperatures. According to calorimetric investigations (Griko et al. 1989), the temperature of maximum stability is near 30 °C under these conditions. The temperature dependence of the Stokes' radius was measured between 30 °C and 2.5 °C. The Stokes' radius at 30 °C, $R_S = (3.01 \pm 0.04)$ nm, is almost the same as under native conditions. A remarkable change in the molecular size was observed at temperatures below 20 °C, reflecting the cold denaturation of the protein. The midpoint of this temperature transition T_M is at 10.5 °C. The unfolding of the protein is nearly complete at 2.5 °C. The Stokes' radius at 2.5 °C is (5.13 ± 0.10) nm. Therefore, the relative increase in R_S at 2.5 °C is about 70% compared to the most compact state at 30 °C. The process of unfolding and subsequent refolding was found to be essentially reversible, as can be concluded from the value of the Stokes' radius of (3.06 ± 0.04) nm at 30 °C after such an experiment. It would be interesting to compare the increase in the molecular size observed during cold denaturation with that observed during heat denaturation at temperatures of about 40 °C. Unfortunately, such attempts have been unsuccessful up to now because heat denaturation was accompanied by a remarkable, mostly irreversible aggregation of protein molecules. Protein aggregation was sensitively indicated by an increase in the total scattered intensity. Some relevant data concerning the change in the molecular size are summarized in Table 1.

Kinetics of the unfolding-refolding reactions

At the beginning of a kinetic experiment, a T-jump from the initial temperature T_i to the final temperature T_f was applied. This T-jump was performed in the following way. The sample cell was carefully flushed with filtered solvent and then mounted in the thermostated cell holder without removing the filter. The sample cell was held at the final temperature T_f. About 0.5 ml of the protein solution was incubated in a syringe at the initial temperature T_i. At the beginning of the experiment, the protein solution was rapidly injected through the filter into the scattering cell. Because of the small cell volume (100 µl), the injected solution should rapidly adopt the temperature T_f. The time constant of this process was estimated by monitoring the translational diffusion coefficient of lysozyme. The Stokes' radius of lysozyme does not change in the temperature range between 5 °C and 30 °C. Therefore, the apparent diffusion coefficient D_{app} immediately displays any changes in T (and $\eta(T)$) according to the Stokes-Einstein equation. A solution of lysozyme was divided into two parts. The cell was filled with one part of the solution and D_{app} was continuously monitored at 5 °C with a data acquisition time of 4.2 s. The second part of the solution, which was stored at 30 °C, was injected at a certain time. The recovery of D_{app} to its value before the injection displays the change in temperature. This is shown in Fig. 2. The time constant is about 20 s. Accordingly, the dead time of this rather simple technique is somewhat larger than the attainable data acquisition time, but it is short enough for the experiments reported below.

Data acquisition and storage during a kinetic experiment is under control of a program written in Turbo Pascal. This program controls the correlator, performs the normalization of the correlation functions, stores the correlation functions on a disk, and displays the time course of an estimate of D_T and the scattered intensity on the monitor screen. Primary data of kinetic experiments are shown in Fig. 3 and Fig. 4. The values of D_T, displayed during an experiment, are calculated by a cumulant fit (Koppel 1972). This rough estimate is sufficient to decide whether D_T is still changing or not. An experiment is stopped either automatically after a pre-selected number of data acquisitions or by hand if D_T reaches a steady state value. For the investigations which are presented here, data acquisition times between 4.2 s and 34 s were chosen. The maximum number of correlation functions registered in one experiment did not exceed 250. This corresponds to data sets of about 400 kByte. Final data evaluation was done after the experiment using the program CONTIN (Provencher 1982 a, b). To run one data set on the transputer takes about 45 s. This computation time is still too long for an on-line calculation of D_T or R_S during a running experiment.

To measure the time constants of the unfolding and refolding processes of PGK, we have performed T-jump experiments between 30 °C, the temperature of maximum stability, and 5 °C, where the protein molecules are predominantly unfolded. The time courses of D_T and of the total scattered intensity I for the unfolding at $T_f = 5$ °C ($T_i = 30$ °C) and refolding at $T_f = 30$ °C ($T_i = 5$ °C) are

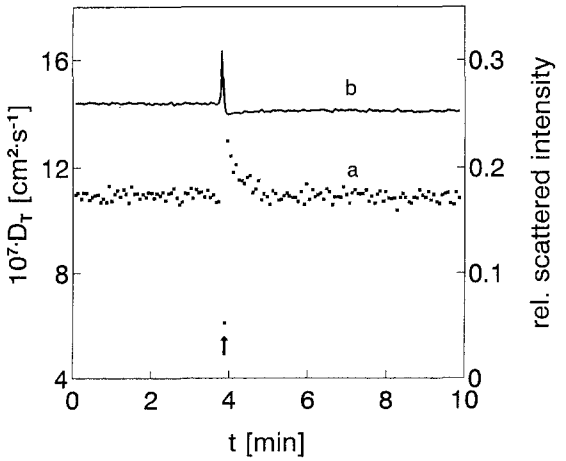

Fig. 2. Time course of the apparent diffusion coefficient D_{app} **a** and scattered intensity **b** for lysozyme, $c = 3.6\ g \cdot l^{-1}$, in 0.3 M glycine-HCl, pH 2.2, 0.15 M NaCl, at $T = 5\,°C$. About 0.5 ml of the solution was pre-incubated at 30 °C and injected at a certain time (arrow). The recovery of D_{app} to the steady-state value at 5 °C displays the equilibration of the temperature. The first record after injection is distorted due to transient inhomogeneities in the index of refraction right after injection

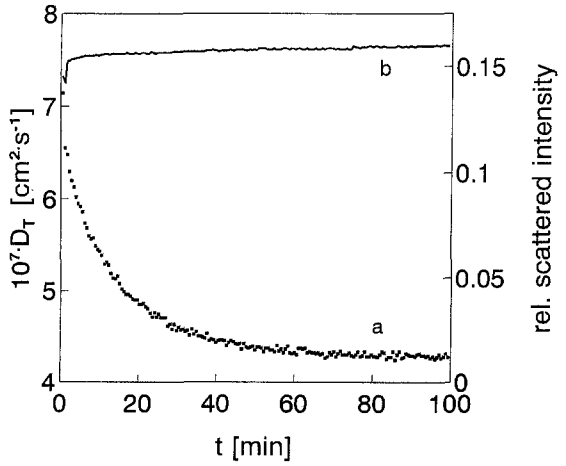

Fig. 3. D_T **a** and scattered intensity **b** versus time during unfolding of yeast PGK, $c = 1.7\ g \cdot l^{-1}$, in buffer plus 0.7 M GuHCl after a *T*-jump from 30 °C to 5 °C

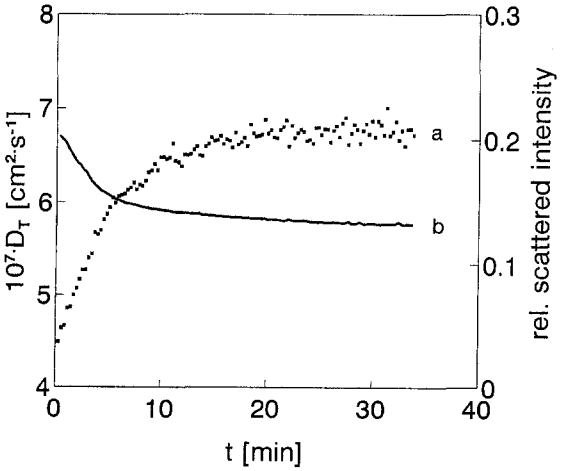

Fig. 4. D_T **a** and scattered intensity **b** versus time during refolding of yeast PGK, $c = 1.7\ g \cdot l^{-1}$, in buffer plus 0.7 M GuHCl after a *T*-jump from 5 °C to 30 °C

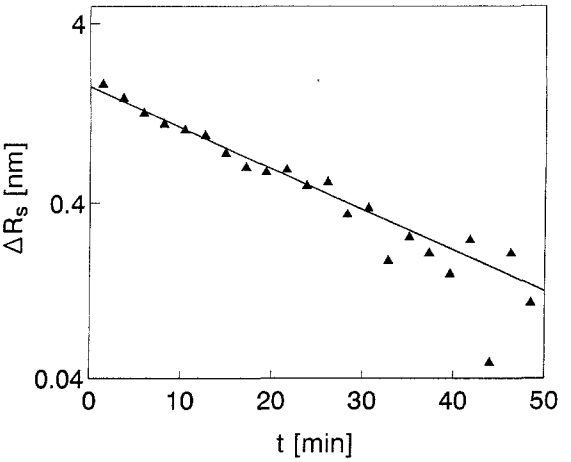

Fig. 5. Logarithmic plot of $\Delta R_S(t) = R_S(\infty) - R_S(t)$ versus time *t* after a *T*-jump from 30 °C to 5 °C. A linear least-squares fit of the data yields the time constant of unfolding of 19 min

shown in Fig. 3 and Fig. 4, respectively. The experiments were performed with a time resolution of 34 s for the unfolding reaction and 17 s for the refolding reaction. Plotting either $\Delta R_S(t) = R_S(t) - R_S(\infty)$ (for refolding) or $\Delta R_S(t) = R_S(\infty) - R_S(t)$ (for unfolding) on a logarithmic scale versus time after the *T*-jump, a nearly linear dependence was observed in both cases. This is shown in Fig. 5 for the unfolding at 5 °C. $R_S(\infty)$ are the steady state values, reached after sufficiently long times *t*. The time constants for unfolding (T_{unf}) and refolding (T_{ref}) have been estimated by a forced least-squares fit of $\ln(\Delta R_S(t))$ to a straight line. We have made this restriction to a first-order process because $\Delta R_S(t)$ deviates only slightly from a single exponential within the experimental error. Fitting the data by a multimodal model may yield unreliable results in such a case. According to T_{ref} (30 °C) = 4.3 min and T_{unf} (5 °C) = 19 min, refolding at 30 °C appears to be considerably faster then unfolding at 5 °C. As can be seen in Fig. 3, only a slight increase in the scattered intensity was observed during unfolding. Possible reasons for this increase could be: the change in the light-scattering constant *K*, the preferential binding of GuHCl or the formation of trace amounts of protein associates. A more complex time course of the scattered intensity was observed during refolding. Immediately after the *T*-jump, the scattered intensity increased very fast to a value somewhat higher than in the unfolded state and then decreased slowly with a time constant comparable to T_{ref} to a value essentially equal to that before unfolding (Fig. 3). This transient increase in the scattered intensity was a common feature of all our refolding experiments. It was more or less pronounced but apparently independent of protein concentration within the investigated concentration range between 0.8 g/l and 2.0 g/l.

Furthermore, we could not detect any concentration dependence of the measured time constants. At times $t \gg T_{ref}$, both the Stokes' radius and the scattered intensity approach the corresponding values before unfolding and subsequent refolding. This gives evidence for the absence of protein associates at the end of the unfolding-refolding reaction. The transient increase in the scattered intensity

is most probably caused by a reversible association of protein molecules during refolding. This working hypothesis is based on the assumption that the unfolded protein chain has an enhanced tendency to associate when it is brought into conditions where the folded native structure is most stable.

The time constant for refolding is of the same order of magnitude as the half-time of refolding of about 2 min for GuHCl denatured yeast PGK at 20 °C measured by fluorescence and absorption difference spectroscopy (Semisotnov et al. 1991). Similar long relaxation times have also been found in unfolding-refolding reactions of a mutant of phage T4 lysozyme at low temperatures (Chen et al. 1989).

Conclusions

The results of our investigations demonstrate that DLS can be successfully applied to the study of unfolding-refolding reactions of protein molecules. The time resolution is in the range of a few seconds according to theoretical estimations assuming typical experimental conditions. This has been verified also by the reported experiments. DLS is particularly useful for investigations of the low-temperature unfolding and refolding of proteins. The time constants of these processes are in the range of seconds or minutes. A more detailed discussion of the investigations on yeast PGK, also including the results of other methods, will be presented in a subsequent paper.

Acknowledgements. The authors are indepted to Mr. B. Grützke for his contribution in developing the correlation technique and to Mrs. D. Otto for skilful technical assistance. We are grateful to Prof. K. Schätzel, Universität Kiel, for kindly providing a preprint of unpublished work. This work was supported by a grant from the Bundesministerium für Forschung und Technologie (BMFT 0319661A) and by grants from the Deutsche Forschungsgemeinschaft (Da 292/1-1) and the Fonds der chemischen Industrie to G. D.

References

Adams B, Burgess RJ, Pain RH (1985) The folding and mutial interaction of the domains of yeast 3-phosphoglycerate kinase. Eur J Biochem 152:715–720

Chen BL, Baase WA, Schellman JA (1989) Low-temperature unfolding of a mutant of phage T4 lysozyme. 2. Kinetic investigations. Biochemistry 28:691–699

Chu B (1974) Laser Light Scattering. Academic Press, New York

Cummins HZ, Pike ER (1974) Photon Correlation and Light Beating Spectroscopy. Plenum, New York

Damaschun G, Damaschun H, Gast K, Gernat C, Zirwer D (1991) Acid denatured apocytochrome c is a random coil: evidence from small angle X-ray scattering and dynamic light scattering. Biochim Biophys Acta 1078:289–295

Dathe M, Gast K, Zirwer D, Welfle H, Mehlis B (1990) Insulin aggregation in solution. Int J Peptide Protein Res 36:344–349

Deverill I, Lock RJ (1983) Kinetics of antigen:antibody reaction. Ann Clin Biochem 20:224–226

Gast K, Zirwer D, Ladhoff AM, Schreiber J, Koelsch R, Kretschmer K, Lasch J (1982) Auto-oxidation induced fusion of lipid vesicles. Biochim Biophys Acta 686:99–109

Gast K, Zirwer D, Welfle H, Bychkova VE, Ptitsyn OB (1986) Quasi-elastic light scattering from human alpha-lactalbumin: comparison of molecular dimensions in native and molten globule states. Int J Biol Macromol 8:231–236

Georgalis Y, Zuoni A, Saenger W (1992) Dynamics of protein precrystallization cluster formation. J Crystal Growth 118:360–364

Griko YV, Venyaminov SY, Privalov PL (1989) Heat and cold denaturation of phosphoglycerate kinase (interaction of domains). FEBS Lett 244:276–278

Harding SE, Sattelle DB, Bloomfield VA (1992) (eds.) Laser light scattering in biochemistry. Royal Society of Chemistry, Thomas Graham House, Cambridge U.K.

Jaenicke R (1987) Folding and association of proteins. Progr Biophys Molec Biol 49:117–237

Jaenicke R (1991) Protein folding: Local structures, domains, subunits, and assemblies. Biochemistry 30:3147–3161

Jakeman E, Pike ER, Swain S (1971) Statistical accuracy in the digital autocorrelation of photon counting fluctuations. J Phys A 4:517–534

Kojro Z (1990) Influence of statistical errors on size distributions obtained from dynamic light scattering data. Experimental limitations in size distribution determinations. J. Phys A 23:1363–1383

Koppel DE (1972) Analysis of macromolecular polydispersity in intensity correlation spectroscopy: the method of cumulants. J Chem Phys 57:4814–4820

Kuwajima K, Sakuruaka A, Fueki S, Yoneyama M, Sugai (1988) Folding of carp parvalbumin studied by equilibrium and kinetic circular dichroism spectra. Biochemistry 27:7419–7428

Laemmli UK (1970) Cleavage of structural proteins during the assembly of the head of bacteriophage T4. Nature 227:680–685

Laggner P, Kriechbaum M, Rapp G (1991) Structural intermediates in phospholipid phase transitions. J Applied Cryst 24:836–842

Mikol V, Hirsch E, Giegé R (1989) Monitoring protein crystallisation by dynamic light scattering. FEBS Lett 258:63–68

Nicoli DF, Benedek GB (1976) Study of thermal denaturation of lysozyme and other globular proteins by light scattering spectroscopy. Biopolymers 15:2421–2437

Pecora R (1985) (ed.) Dynamic Light Scattering: applications of photon correlation spectroscopy. Plenum, New York

Privalov PL (1990) Cold denaturation of proteins. Critical Reviews in Biochem. and Molecular Biology 25:281–305

Provencher SW (1982a) A constrained regularization method for inverting data presented by linear algebraic or integral equations. Comp Phys Commun 27:213–227

Provencher SW (1982b) CONTIN: A general purpose constrained regularization program for inverting noisy linear algebraic and integral equations. Comp Phys Commun 27:229–242

Schätzel K (1983) Noise in photon correlation and photon structure functions. Optica Acta 30:155–166

Schätzel K (1987) Correlation techniques in dynamic light scattering. Appl Phys B 42:193–213

Schätzel K, Drewel M, Stimac S (1988) Photon correlation at large lag times: improving statistical accuracy. J Modern Optics 35:711–718

Schätzel K (1990) Noise in photon correlation data: I. Autocorrelation functions. Quantum Opt 2:287–305

Schätzel K (1992) Single photon correlation techniques. In: Brown W (ed.) Photon correlation spectroscopy, the method and some applications. Oxford University Press, Oxford, in press

Schmitz KS (1990) An introduction to dynamic light scattering. Academic Press, Boston

Semisotnov GV, Vas M, Chemeris VV, Kashparova NJ, Kotova NV, Razgulyaaev OI, Sinev MA (1991) Refolding kinetics of pig muscle and yeast 3-phosphoglycerate kinases and of their proteolytic fragments. Eur J Biochem 202:1083–1089

Sluzky V, Tamada JA, Klibanov AM, Langer R (1991) Kinetics of insulin aggregation in aqueous solutions upon agitation in the presence of hydrophobic surfaces. Proc Natl Acad Sci USA 88:9377–9381

Tanford C (1961) Physical chemistry of macromolecules. Wiley, New York

Watson HC, Walker NPC, Shaw PJ, Bryant TN, Wendell PL, Fothergill LA, Perkins RE, Conroy SC, Dobson MJ, Tuite MF, Kingsman AJ, Kingsman SM (1982) Sequence and structure of yeast phosphoglycerate kinase. EMBO J 1:1635–1640